Journal of Materials Chemistry B

ROYAL SOCIETY OF CHEMISTRY

REVIEW

View Article Online
View Journal | View Issue

Cite this: *J. Mater. Chem. B*, 2022, **10**, 7460

Nucleic acid paranemic structures: a promising building block for functional nanomaterials in biomedical and bionanotechnological applications

Jung Yeon Lee,† Qi Yang,† Xu Chang, Henry Wisniewski, Tiffany R. Olivera, Minu Saji, Suchan Kim, Devanathan Perumal and Fei Zhang *

Received 21st March 2022,
Accepted 19th July 2022

DOI: 10.1039/d2tb00605g

rsc.li/materials-b

Over the past few decades, DNA has been recognized as a powerful self-assembling material capable of crafting supramolecular nanoarchitectures with quasi-angstrom precision, which promises various applications in the fields of materials science, nanoengineering, and biomedical science. Notable structural features include biocompatibility, biodegradability, high digital encodability by Watson–Crick base pairing, nanoscale dimension, and surface addressability. Bottom-up fabrication of complex DNA nanostructures relies on the design of fundamental DNA motifs, including parallel (PX) and antiparallel (AX) crossovers. However, paranemic or PX motifs have not been thoroughly explored for the construction of DNA-based nanostructures compared to AX motifs. In this review, we summarize the developments of PX-based DNA nanostructures, highlight the advantages as well as challenges of PX-based assemblies, and give an overview of the structural and chemical features that lend their utilization in a variety of applications. The works presented cover PX-based DNA nanostructures in biological systems, dynamic systems, and biomedical contexts. The possible future advances of PX structures and applications are also summarized, discussed, and postulated.

Introduction

In the last several decades, DNA has been used as a building material for a variety of nanostructures, such as one-dimensional (1D) arrays,[1,2] two-dimensional (2D) arrays and shapes,[3–6] and three-dimensional (3D) nanostructures.[7,8] These nanostructures have been adopted in a variety of both biomedical[9–14] and biotechnological[15,16] applications. The popularity of using DNA as a nanomaterial is attributed to its predictable secondary structure, biocompatibility, and nanoscale manipulation. The highly predictable and programmable nature of DNA lies in the

Department of Chemistry, Rutgers University, Newark, NJ 07102, USA.
E-mail: fei.zhang@rutgers.edu; Tel: 973-353-5520
† Equal contributions.

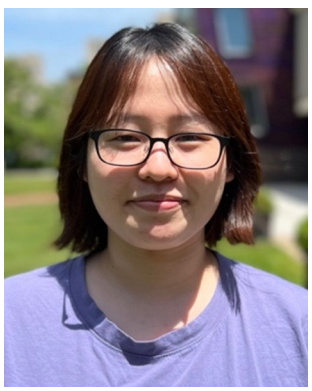

Jung Yeon Lee

Jung Yeon Lee is currently a PhD student in the Department of Chemistry at Rutgers University Newark campus. She received her MA in Chemistry at University of Maryland at Baltimore County in 2018 and BS in Pharmaceutical Sciences from the State University of New York at Buffalo in 2016. Her research focuses on the topics of self-assembly of DNA and RNA nanostructures.

Qi Yang

Qi Yang is currently a PhD student in the Department of Chemistry at Rutgers University Newark campus. She received her MS in Chemistry at Shanghai Normal University in 2018 and BS in Chemistry from Anhui Agricultural University in 2014. Her research interests include DNA tile, dynamic DNA nanodevices, higher-ordered assembly of DNA origami, and RNA nanostructures.

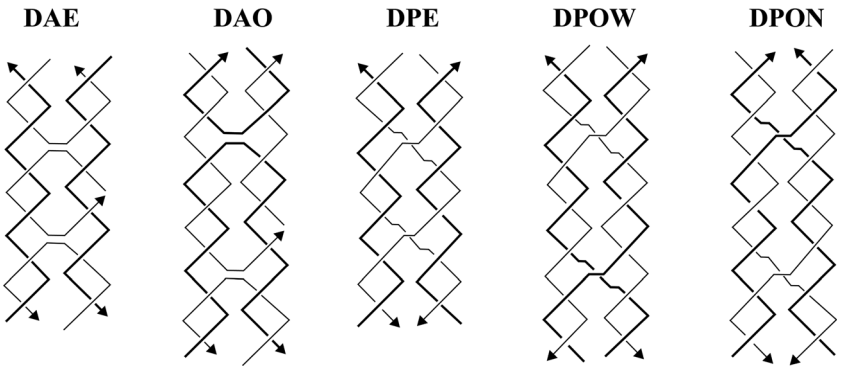

Fig. 1 Five DNA structural motifs with double crossovers or the immobile Holliday junctions. Reproduced with permission from ref. 20. Copyright 1993, Biochemistry.

classic Watson and Crick's base pairing rules.[17] DNA is also biodegradable[18] and biocompatible[19] because it is a native, biological macromolecule that codes for important genetic and hereditary information found in many living organisms.

In 1993, Fu and Seeman introduced immobile Holliday junctions (double crossover DNA motifs, DXs) that were used as building blocks to create rigid and complex nanostructures.[20] With inspiration from the biological, mobile Holliday junctions, which are involved in biological recombination processes, they came up with five different DNA structural motifs: DAE, DAO, DPE, DPOW, and DPON (Fig. 1). The sequences chosen for these were specifically designed to prevent branch migration, thus making them 'immobile' Holliday junctions. These motifs are also called DXs that consist of two DNA helices in close proximity connected by two crossovers. DAE and DAO motifs (DAs) are designated with 'A' because their crossover strands are oriented in an 'antiparallel' direction, whereas DPE, DPOW, and DPON (DPs) are designated with 'P' because their crossover strands are parallelly oriented. The 'E' and 'O' are abbreviations for 'even' and 'odd' number of helical turns between the two crossovers, respectfully. Finally, 'W' and 'N' from DPOW and DPON refer to the presence of a majority of wide major grooves or a majority of narrow minor grooves near the central dyad axis of the parallel motifs.

Motifs containing antiparallel oriented crossovers (AX) behave more predictably in early studies.[20,21] For this reason, AX motifs have been used more often in building a variety of complex nanostructures from tile arrays[3,4] to 3D nanostructures including origami-based structures with AX crossover staple strands.[7,22] Although PX motifs are less popular than AX motifs, the importance of using PX motifs should not be neglected and require further investigation. Studies of PX motifs so far have revealed that PX motifs have their own unique features endowing them with potential benefits that AX motifs cannot achieve.

One exciting feature of PX motifs is their unique strand routing. PX has been used to explore different strand routing strategies to achieve complex, single-stranded DNA nanostructures. As shown in Fig. 2a, PX motifs can adopt various structural forms ranging from multi-stranded motifs varying in crossover positions to a single-stranded PX motif.[23] The motif labeled with PX is the same as the one labeled PX-N. The only difference between PX-N and PX-W (N, minor groove; W, major groove) is the size of the groove at which the crossover strands are located. DB's indicates a dumbbell motif with two separate, closed double helices that interact to form the paranemic crossovers or the PX. Notably, the entire PX motif can be single-routed to form a single-stranded PX motif that contains intramolecular paranemic crossovers, broadening a new way to construct large, complex nanostructures. For example, Shih *et al.* designed a stable 3D octahedron nanostructure using a 1.7-kilobase single-stranded DNA as a scaffold that contained half-PX segments to allow intramolecular PX connections (Fig. 2b).[8] Seven PX junctions, created from joining two half-PX segments, were intramolecularly bonded after annealing from high to low temperatures to produce the target octahedron structure. Followingly, in 2017, a new technique called single-stranded origami (ssOrigami) has been created to form large, single-stranded PX-based nanostructures.[24] Unlike the

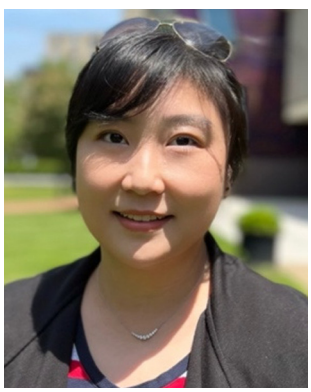

Fei Zhang

Dr. Fei Zhang joined the Chemistry Department at the Rutgers University Newark campus as an Assistant Professor in 2019. She received her BS in Chemistry from Peking University in 2010 and her PhD in Chemistry and Biochemistry from Arizona State University in 2015. Dr Zhang's work was recognized with the Robert Dirks Molecular Programming Prize. In 2021, she received the NSF Faculty Early Career Development (CAREER) award. Dr Zhang's research efforts are focused on advancing the fundamental design and creation of new functionalities and enabling diverse applications of highly programmable nucleic acid nanostructures.

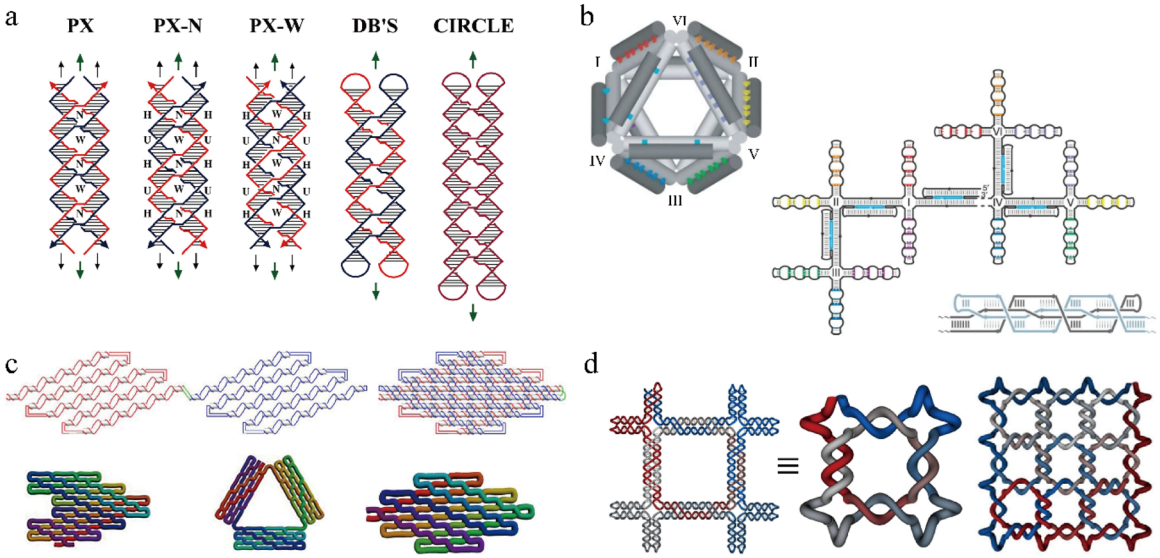

Fig. 2 Representative PX-based DNA nanostructures. (a) Schematic drawings of paranemic crossover DNA tiles and its closed analogues. (b) A 3D octahedron nanostructure with seven intramolecular paranemic junctions. (c) Three unknotted single-stranded origami nanostructures. (d) One representative single-stranded DNA knots based on PX. Reproduced with permission from ref. 23. Copyright 2004, Journal of the American Chemical Society. Reproduced with permission from ref. 8. Copyright 2004, Nature. Reproduced with permission from ref. 24. Copyright 2017, Science. Reproduced with permission from ref. 25. Copyright 2018, Nature Communications.

conventional method using a multicomponent, scaffolded origami technique,[6] in which a long, scaffold strand is folded into a large, designed nanostructure with the help of hundreds of short staple strands, the ssOrigami do not require any staple strands but form the target structures through intramolecular paranemic interactions. Since the paranemic interactions do not require crossover strands to thread through another interacting helix, the ssOrigami are fully unknotted structures. As shown in the Fig. 2c, a red-half PX domain simply overlays on top of blue-half PX domain without creating any knots with their size up to 10 682 nt. Furthermore, the topological and kinetic traps that were likely to occur during the formation of highly knotted structures can be avoided by applying stepwise folding pathways. For example, in 2018, a set of complex DNA and RNA knots have been assembled by hierarchical folding a single-stranded DNA or RNA chain in a defined order (Fig. 2d).[25] The unique single strand folding pathways of knotted or unknotted PX nanostructures have enabled self-replicating nanostructures through biological methods, demonstrating potentials for low-cost high throughput production of the nanostructures.

In addition, various studies have shown that PX motifs have other potential benefits for biomedical applications such as improved rigidity, low-cost yet time-efficient production, enhanced nuclease resistance, high biostability, high biocompatibility, the ability to perform as dynamic nanodevices, and other important biological relevance. This review paper summarizes the benefits of using PX motifs in DNA nanostructures, highlights the biomedical applications of PX structures, and provides insights into future work to enhance the knowledge of using PX motifs for nanostructures assembly and biomedical applications.

Significance of using PX motifs in biomedical and bionanotechnological applications

The unique structural features of PX motifs, including enhanced structural rigidity due to paranemic interactions, high stability against nuclease degradation, large scale synthesis *via* Rolling Circle Amplification (RCA) makes them a potential candidate for *in vivo* biomedical applications such as drug delivery, bioimaging, and sensing. Furthermore, PX motifs have been shown to play an important role in the homology recognition (HR) process. Therefore, understanding the biological role of PX motifs can provide better insights into HR mechanisms. PX motifs can be incorporated into DNA nanodevices to display dynamic features. Overall, PX motifs hold great promise for various applications in biological/biomedical fields, all of which will be discussed in detail in the following section.

Enhanced rigidity of PX motifs

PX motifs can be used to connect nanostructures either intramolecularly or intermolecularly to form stable 1D and 2D arrays,[1,2,5,26] a 3D shaped nanostructure (*e.g.* octahedron[8]), and other unique structures like DNA rotaxanes[27] and catenated/knotted structures.[28] For example, Kumara *et al.*'s group has achieved a successful two-tile based assembly using a double-crossover PX motif as each tile (Fig. 3a).[29] By introducing favorable folding pathways to each PX motif, they were able to produce successfully folded double-crossover PX motifs, leading to large 2D arrays. Their study provided evidence that adjusting the folding pathway allows the PX motifs to grow into large 2D arrays, highlighting the rigidity and stability of PX motifs. Besides, PX motifs can be the alternative method to the

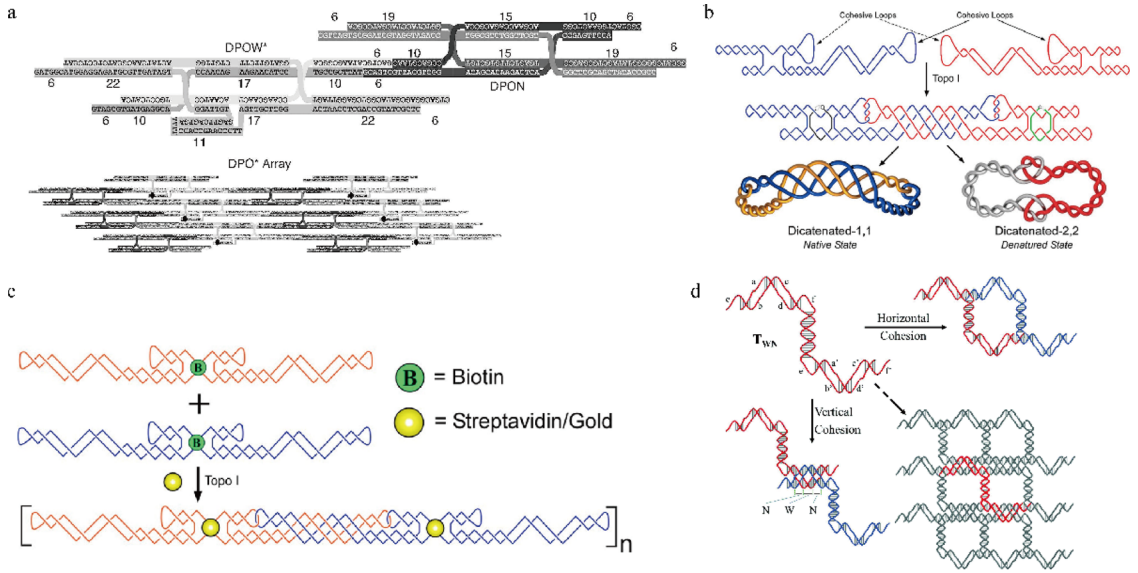

Fig. 3 1D and 2D arrays assembled from rigid PX motifs. (a) The design of DPOW* and DPON tiles and corresponding 2D array. (b) Two single-stranded tiles (blue and red) joined with a PX connection, followed by the formation of catenated structures after topoisomerase I treatment. (c) A two DNA tile-based 1D array *via* paranemic cohesion as a scaffold to direct gold nanoparticles array formation. (d) A 2D array using *Z*-shaped PX tiles with different numbers of bp, assigned to major and minor grooves. Reproduced with permission from ref. 29. Copyright 2008, Nano Letters. Reproduced with permission from ref. 28. Copyright 2015, ACS Nano. Reproduced with permission from ref. 2. Copyright 2015, ACS Nano. Reproduced with permission from ref. 5. Copyright 2016, Organic & Biomolecular Chemistry.

conventional way of using sticky ends for intra/inter molecular cohesion. In comparison, PX motifs can provide more thermostability in cohesion than the use of sticky ends, which are typically between 4–6 nucleotides long and have relatively low melting temperatures. Ohayon *et al.* fabricated two DNA tiles that were joined by PX connections, forming unique structures that were catenated after topoisomerase I treatment (Fig. 3b).[28] These catenated structures not only made the tiles resistant to temperature changes, but also helped them to withstand environments with chemical denaturing agents. In addition, they created a 1D array using two DNA tiles through paranemic cohesion and attached gold nanoparticles, *via* biotin/streptavidin interaction, on each tile (Fig. 3c), leading to gold conjugated 1D arrays formation.[2] A year later, a 2D array using *Z*-shaped PX tiles (Fig. 3d) were constructed by Shen *et al.*[5] The 2D array was formed with paranemic connections in the vertical direction and T-junction connections in the horizontal direction. In this work, Shen *et al.* studied the effects of the number of base pairs (bp) in major and minor grooves in the PX motifs on the 2D array. The same group also found that the tile with six bps in the major groove and five bps in the minor groove (T65) was the most stable motif, producing a large 2D array, whereas other tiles (T55, T75, *etc.*) formed small crystals, linear structures, and aggregates. The hypothesis based on this systematic study was that the structural features of T65 was closest to that of B-form DNA structure, thereby leading to a large array. Their follow-up study confirmed this hypothesis, highlighting the importance of adjusting the number of bps to as close to the B-form DNA as possible.[30] All these studies showed that PX motifs can be used to create rigid intra/intermolecular connections and to improve thermal stability, resistance to chemical denaturing agents, and nuclease degradation.[31] These benefits of PX motifs in creating novel and rigid nanostructures can be highly valuable in biomedical applications.

Scalable enzymatic amplification of PX motifs

The large-scale synthesis of target nanostructures is highly crucial when it comes to industrial applications. Therefore, cost and time are important factors to consider while choosing the appropriate fabrication methods to synthesize the nanostructures. Even though standard phosphoramidite chemistry[32] allows the synthesis of both natural as well as modified oligonucleotides, this method is costly especially for large-scale production and for long single-stranded DNAs (typically more than 100 nucleotides) that can be easily achieved using PX motifs. Lin *et al.* introduced and investigated an alternative strategy called Rolling Circle Amplification, RCA, (Fig. 4a) to synthesize a single-stranded DNA nanostructure containing multiple PX crossovers *in vitro*.[33] In this study, the starting PX motif with multiple crossovers was initially made into a circle by a circle-ligase and then enzymatically amplified by a DNA polymerase. After amplification, a long final product containing copies of PX motifs was formed and then cleaved by restriction digestion into multiple copies of the target structures. The RCA could then be repeated with an increasing number of cycles, leading to exponential amplification of the target PX motifs. Furthermore, the group had identified several parameters with this technique such as: the length of primer for polymerase binding, the formation of by-products, and the restriction digestion conditions. They also suggested that optimizing these variables could further improve the efficiency of RCA. This simple, time- and cost-effective technique can be

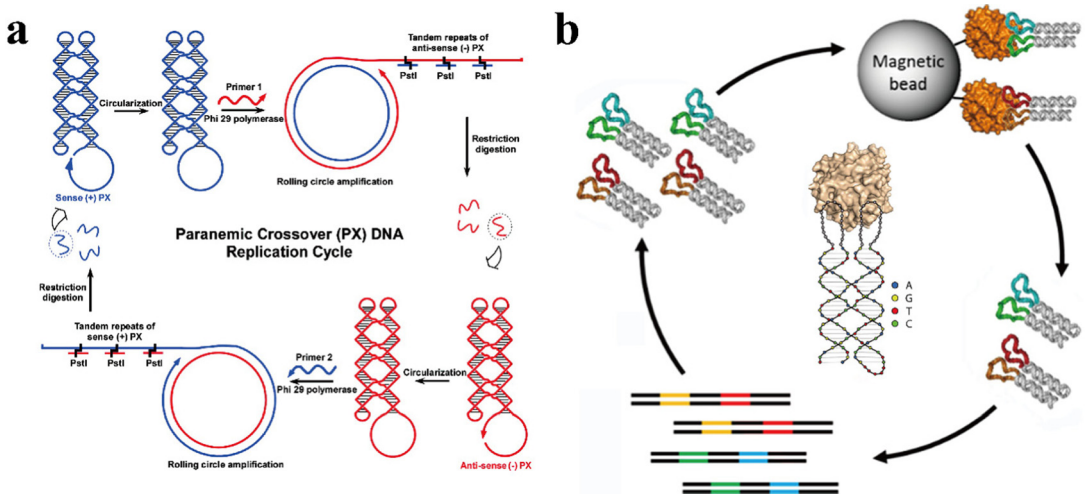

Fig. 4 Self-replicating PX motifs. (a) The cycle of RCA starts with a single-stranded PX motif (blue) in the first phase and repeats with a primer 2 in the second phase with the copied PX motifs (red) from the first phase. (b) Bivalent aptamers of human α-thrombin generated from PX-based DNA nanostructures through a SELEX procedure. Reproduced with permission from ref. 33. Copyright 2007, Journal of American Chemical Society. Reproduced with permission from ref. 36. Copyright 2019, Chembiochem.

applied for amplification of higher-ordered, complex PX structures that can self-fold.[34] In addition, such enzymatic replication can also be performed with the use of helper phages infecting *E. coli* cells for enhanced amplification.[34,35] To make RCA and the cellular amplification even more affordable, catalytic DNAs or deoxyribozymes have been introduced as a cost-effective alternative to the restriction enzymes for cleaving/extracting the amplified target single-stranded PX motifs in a large quantity.[34]

Besides RCA and the cellular amplification, the Systematic Evolution of Ligands by Exponential Enrichment, SELEX, technique has been introduced to generate bivalent aptamers by employing single-stranded PX containing oligonucleotide.[36] Aptamers with high binding affinity with a femtomolar-range to the target protein, thrombin, have been selected. As shown in Fig. 4b, a large DNA library containing 10^{15} single-stranded DNA (ssDNA) oligos, containing defined structural regions to fold into PX motifs and two loop regions of random sequences. During the SELEX process, aptamers bind with thrombin through the two sites of interaction between each loop region of the aptamers and each of two different thrombin epitopes (exocite I and II). The thrombin bound with specific aptamers can be magnetically separated out, and the aptamers are isolated from the thrombin during the elution process. These aptamers can further be amplified using polymerase chain reaction (PCR) and undergo a few more rounds of the same SELEX procedures to selectively sort out the aptamers with the highest binding affinity towards thrombin. After multiple rounds of SELEX process, the aptamer with the highest binding affinity is identified and amplified in a large quantity. This study shows that the selected aptamer containing PX crossovers not only can be amplified *via* SELEX but also show femtomolar-range affinity towards thrombin with the help of bivalent interaction (two loop interaction with two epitopes). Furthermore, such aptamer with highest affinity towards thrombin produced strong anticoagulant effect through the allosteric modulation of thrombin activity. Based on studies discussed in this section, using PX motifs allowed the formation of single-stranded nanostructures, which can be amplified into a large quantity using affordable methods such as RCA, cellular amplification, and SELEX/PCR. Particularly for the single-stranded aptamers used in SELEX, PX motifs allowed strong, bivalent interaction with the target protein by intramolecularly joining two helical segments, each of which contains the target-binding loop. Such aptamers combined with PX motifs exhibit high affinity and specificity towards target proteins and can be used to modulate malfunctioning protein activities, highlighting the potential benefit of using PX motifs in such biomedical application.

Biocompatibility, biostability, and nuclease resistance of PX-based nanostructures

DNA-based nanostructures have been specifically designed to cage drug molecules and deliver them to targets, like diseased cells, and perform as smart drug carriers.[10,11] In addition, these nanostructures also perform as biosensors[14,37] and bioimagers.[11,13,38] One of the challenges in fabricating these nanostructures for *in vivo* applications is degradation by DNA nucleases that are ubiquitous in biological environments (*e.g.* saliva, urine, and blood) that destroy nucleic acid-based vehicles.[39] To work as an effective drug delivery vehicle, biosensor, or bioimager, DNA nanostructures should be able to survive such complex biological environments before reaching the target cells.

In 2020, Chandrasekaran *et al.*'s research group investigated the effects of adding PX crossovers in DNA on the DNA's nuclease resistance regions in biological systems.[40] They used a **PX 6:5** molecule (Fig. 5a) as their model containing six nucleotides and five nucleotides in the major (W or wide) and minor (N or narrow) grooves, respectively. **PX 6:5** molecule was incubated with various nuclease enzymes such as DNase I, T7

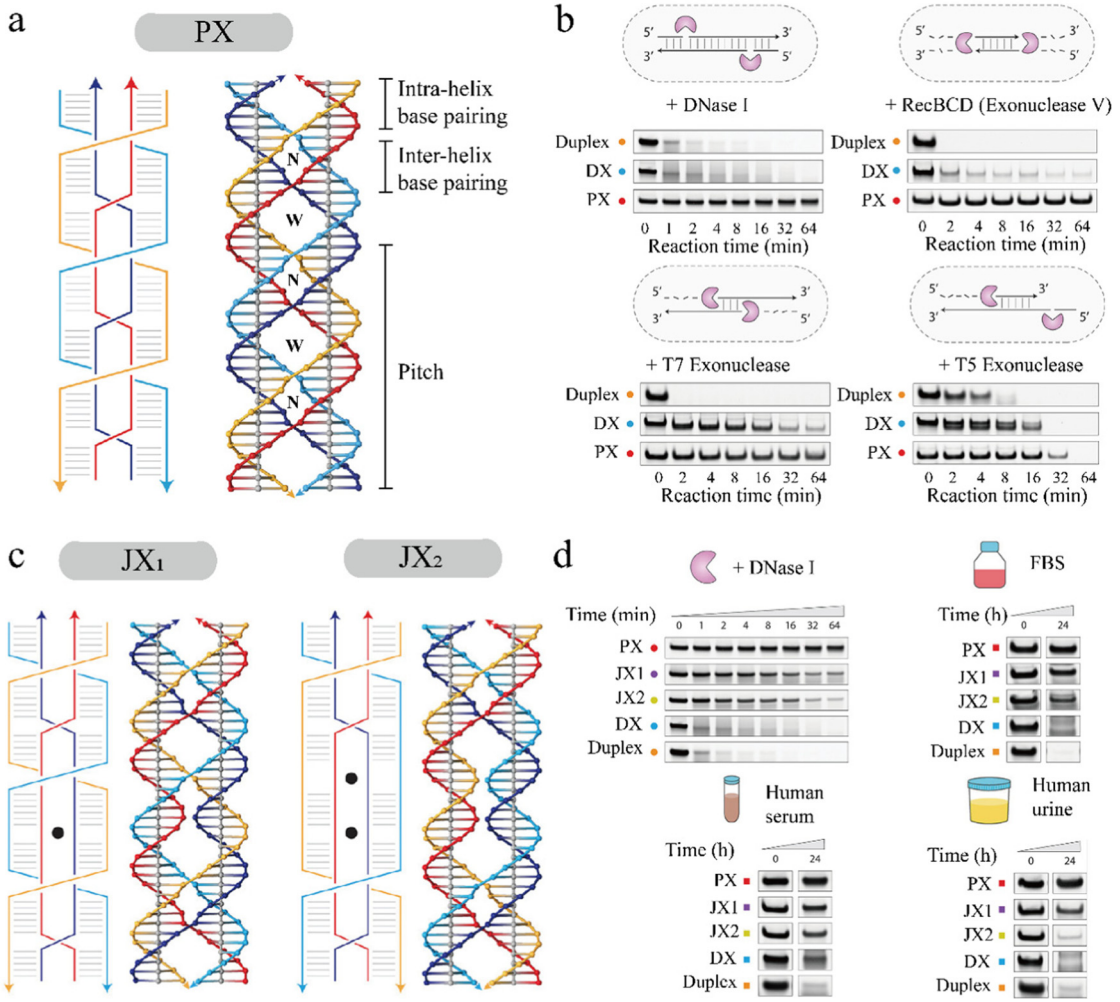

Fig. 5 Design of PX tiles and PX tiles analogs (JX, with fewer crossovers), and investigation of crossover-dependent biostability. (a) **PX 6 : 5** motif with six nucleotides in major grooves and five nucleotides in minor grooves. (b) Nuclease resistance of the **PX 6 : 5** motif, DX (a PX motif with two crossovers), and duplex (a double-stranded DNA) tested with four types of nucleases, DNase I, RecBCD, T7 exo, and T5 exo. (c) JX1 and JX2 motifs produced from **PX 6 : 5** by removal of one or two crossovers, respectively. (d) The crossover-dependent degradation trend of PX, JX1, JX2, DX, and duplex in DNase I, FBS, human serum, and human urine, respectively. Reproduced with permission from ref. 40. Copyright 2020, Journal of the American Chemical Society.

and T5 exonucleases, and Rec BCD. As shown in Fig. 5b, they quantified the degradation of the **PX 6 : 5** by measuring band reduction in polyacrylamide gels and comparing it with controls like duplex DNA and a DX motif containing only two PX crossovers. In 0.1 units of DNase I solution, over 90% of the duplex and DX structures were degraded quickly in just a few minutes, whereas less than 5% of the **PX 6 : 5** was degraded after one hour, showing its superior nuclease resistance. Similarly, tests with other nucleases, Rec BCD, T7, and T5 exo, revealed that **PX 6 : 5** exhibited higher resistance to nuclease degradation. Based on this finding, Harvorsen's group hypothesized that the number of PX crossovers added to a DNA motif is directly proportional to the degree of nuclease resistance by the DNA motif.[40] To test this hypothesis, they created PX tiles analogs (JX1 and JX2) that have fewer number of crossovers compared to the **PX 6 : 5** containing six crossovers. **JX_1** had five crossovers, whereas **JX_2** had four crossovers (Fig. 5c). Next, they performed similar gel analysis to quantify the reduction in the bands of target structures after incubating the structures with 0.1 units of DNase I. The gel quantification result (Fig. 5d) showed that the **PX 6 : 5** had the highest resistance to DNase I as predicted, followed by **JX_1**, **JX_2**, DX, and duplex in decreasing order of nuclease resistance. This result confirmed that the number of PX crossovers is crucial in resisting nuclease degradation.

Furthermore, they performed MTT (3-(4, 5-dimethylthiazolyl-2)-2, 5-diphenyltetrazolium bromide) assays to test the potential cellular interference of **PX 6 : 5** by incubating it in mouse C2C12 myoblasts and human HeLa cell lines. The experimental results showed that **PX 6 : 5** has biocompatibility and did not induce changes in the cellular differentiation process. Next, they tested the biostability of PX tiles in other three kind of biological fluids, including fetal bovine serum (FBS), human serum, and human urine, compared with JX_1, JX_2, DX, and duplex. Similar to the trend of crossover-dependent nuclease resistance, **PX 6 : 5** exhibited the highest biostability with the least degradation over 24 h

incubation in the selected biological fluids as shown in Fig. 5d. JX_1, JX_2, DX, and duplex showed an increase in nuclease degradation with a decrease in the number of PX crossovers, confirming that biostability in the biological fluids is also crossover dependent.

Dynamic nanodevice by incorporating PX motifs

PX motifs can be used as a dynamic nanodevice, achieving various tasks such as input-output computation, carrying cargos, arm movement, and assembly of polymers. Many DNA-based dynamic devices that undergo changes in their shapes upon exposure to various stimuli, including pH,[41] ions concentration,[42] temperature,[43] light,[44] and protein[45] have been created so far. Another important stimulus is DNA strands, or fuel strands. Dynamic motion generated in response to fuel strands is known to be driven by toe-hold-mediated strand-displacement reactions or branch migration.[46] This type of sequence-dependent reaction has been performed in previous studies.[46–49] Compared to the previous sequence-dependent devices, the PX-based device has been applied in more practical applications such as computation, cargo/arm movement, and polymer assembly. The fundamental basis of all PX-based nanodevices is the use of the two-state **PX-JX$_2$** rotary device, which rotates by 180 degrees between the two-states (Fig. 6a).[50] In this study, important terms such as fuel strands and set strands were introduced. As the names themselves imply, fuel strands (the 'green' or 'purple' colored ssDNAs) refer to the strands that initiate conformational change between **PX** and **JX$_2$** *via* toe-hold-mediated strand displacement. The set strands (the 'green' or 'purple' colored strands hybridized within the **PX** and **JX$_2$** systems) are the strands that lock the state of the device in either **PX** or **JX$_2$** conformation and contain extra, unpaired, overhanging sequences to bind the fuel strands. This extra-base pairing between the fuel strands and set strands is the driving force for the strand displacement reaction. Using 'n' different **PX-JX$_2$** rotary devices produce 2^n structural states, allowing large-scale applications. Later, a three-state device was introduced based on the two-state device, further increasing the possible number of states to 3^N.[51] Multiple **PX-JX$_2$** devices were used to create polymers, as well as to produce a specific output. In the two studies,[52,53] the rotating motion of **PX** and **JX$_2$** motifs controlled the binding of different input strands with their designed systems, thereby producing different types of polymers, a long DNA strand that could be conjugated with a functional polymer of interest, and output tiles. In Fig. 6b, six different DX motifs (DX2-7) were designed to bind the **PX**/**JX$_2$** system through sticky-ends interactions. The orientation of the system *via* switching between **PX** and **JX$_2$** generated a variety of DNA polymers with different sequences.[52] In Fig. 6c, externally added tiles bound to the system through sticky-ends

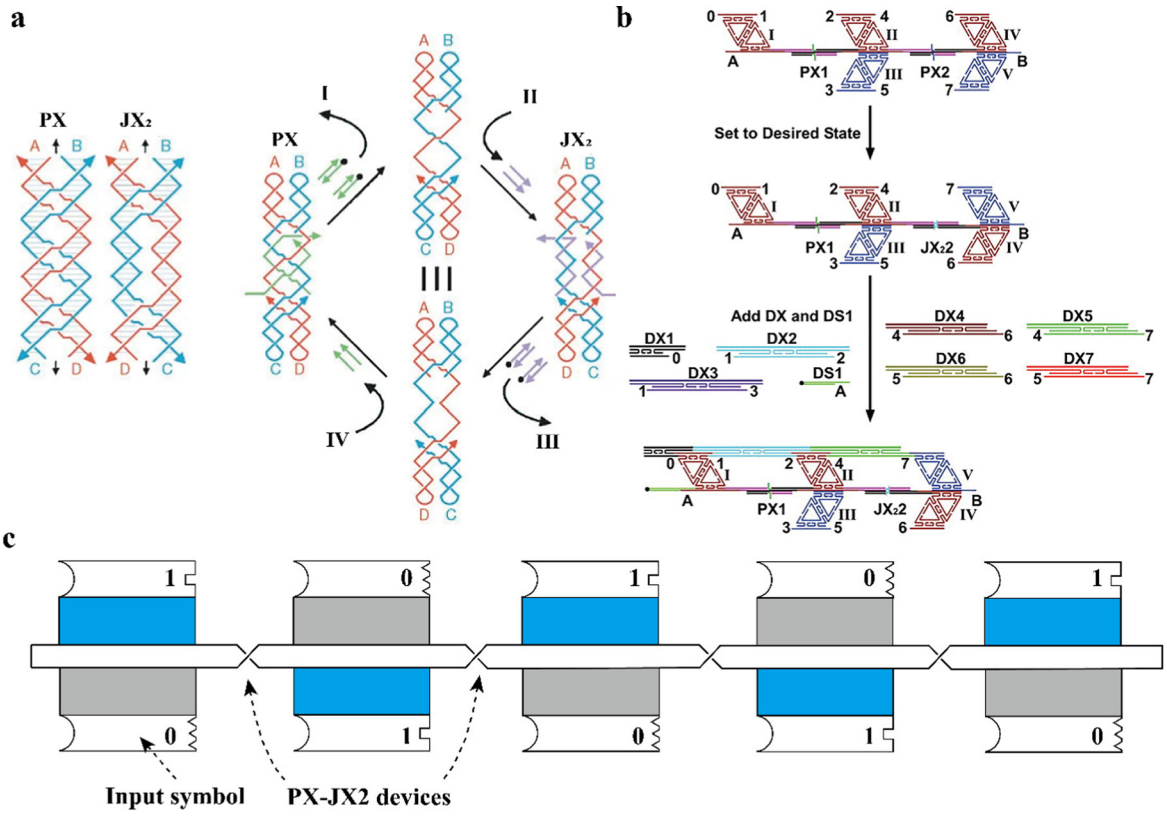

Fig. 6 Dynamic nanodevices based on PX motifs. (a) A two-state **PX-JX$_2$** rotary device that rotates by 180 degrees between the two-states, **PX** and **JX$_2$**. (b) A schematic representation of polymer assembly pathway using **PX-JX$_2$** devices (c) A schematic representation of a computational input and output system using **PX-JX$_2$** devices Reproduced with permission from ref. 50. Copyright 2002, Nature. Reproduced with permission from ref. 52. Copyright 2004, Science. Reproduced with permission from ref. 53. Copyright 2012, Chemical Science.

interactions labelled with a '0' or a '1' and the **PX/JX$_2$** switch controlled the relative orientations of the sticky ends, leading to different output products.[53] Other examples using **PX-JX$_2$** devices include a DNA robot arm (a dynamic arm rotation)[54] and a nanoscale assembly line (cargo movement).[55] All these studies show the versatility of a **PX-JX$_2$** device in creating dynamic, practical DNA nanodevices.

PX motifs in homology recognition

Studies so far have suggested that PX motifs might be involved in recombination-independent homologous pairing (RIHP),[56] important biological processes of fungi,[57] mammalian cells,[58] insects,[59] plants,[60] and most importantly in humans.[61] Failure in homologous pairing is known to produce errors in chromosome segregation during meiosis in humans, leading to aneuploidy, posing harmful effects on newborn babies. Previously, efforts have been made to characterize homologous pairing (HP) events that occurred under physiological conditions *in vitro*[62–66] and to develop models[67,68] to explain the process of HP. However, both the HP processes studied *in vitro* and the proposed models had limitations in explaining actual molecular mechanisms that took place *in vivo*, requiring further study. One interesting study by Seeman's group investigated, and confirmed, the formation of PX motifs and the occurrence of PX HP in a negatively supercoiled *E. coli* plasmid (pUC19) both *in vitro* by using the plasmid manipulated with PX homologous sequences (multiples of **PX 6 : 5**) and in cells using Atomic Force Microscopy (AFM) imaging.[56] The *in vitro* AFM images clearly showed a dumbbell-shaped structure with a shaft in the middle, which was explained in their model (Fig. 7a). They suggested that this type of transition from a supercoiled structure to a shaft-containing dumbbell structure might be driven by the relaxation of the supercoiling, leading to a more energetically favorable state with HP. In addition, a recent study by Kizer's group identified a potential *anti*-PX ligand, T7 endonuclease I, that binds PX motifs with high affinity and specificity (Fig. 7b).[69] They indicated that using the *anti*-PX ligand could further validate the formation of PX motifs shown in the AFM image of a shaft-containing structure. All these studies revealed that PX motifs may play a crucial role in RIHP. However, further experiments need to be carried out to further elucidate the mechanism of RIHP *in vivo* using PX homologous pairing. Understanding the PX homology-based mechanism of RIHP can help to realize the importance of RIHP in complex biological processes and the factors influencing RIHP that lead to harmful effects (*e.g.* aneuploidy). The mechanistic studies of PX homology-based RIHP will therefore stimulate the areas of biomedical applications targeting the problems associated with RIHP.

PX-based nanostructures for biomedical applications

In addition to the biostability and cost-efficient scalability, the ability to single route the PX motifs helps to avoid purity and structural integrity issues associated with redundant or missing strands in the target structures, which exhibit great potential for biomedical applications. As mentioned earlier, PX motifs have been used to develop a bivalent aptamer by joining two helices, each of which contains a loop of random sequence, in a single-stranded routing.[36] By performing the SELEX technique, the bivalent aptamer with the highest binding of thrombin was identified. According to the fibrin clotting assay with human plasma, this bivalent aptamer was shown to be a potential candidate ligand as a strong anticoagulant. Another study utilized the PX motifs to form single-stranded DNA nanostructures and investigated their ability to sort liposome efficiently as well as to enhance cellular uptake of the liposome.[34] Liposome has been used to function as an excellent drug delivery vehicle for its safety, selectivity towards target cells through modification on its surface, biostability, and controlled release of drug compounds by increasing their half-lives and shielding them from possible degradation in body.[70] It was previously highlighted that liposomes coated with ssDNA show their potential ability to improve cellular uptake in specific cancer cells.[71] Here, RCA-amplified PX-based single-stranded nanostructures have been conjugated onto liposomes and tested to show efficient sorting to selectively sort out liposomes into an

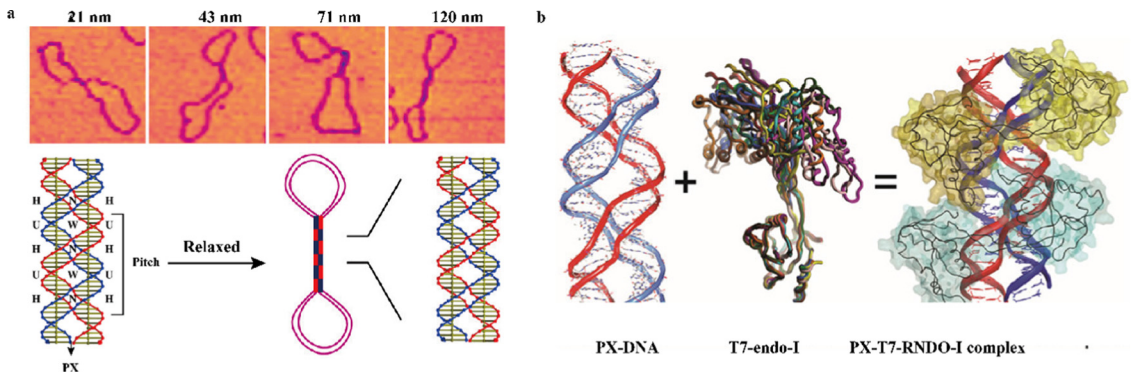

Fig. 7 Representative examples of biological relevance of PX motifs. (a) AFM images showing a dumbbell shaped structure with a shaft in the middle (top). Schematic models explaining and confirming the dumbbell shaped structure formed with PX-homology in a relaxed conformation (bottom). (b) A potential *anti*-PX ligand, T7 endonuclease I (T7-endo-I), that binds PX motifs with high affinity and specificity to form a PX-T7-endo-I complex. Reproduced with permission from ref. 56. Copyright 2010, Proceedings of the National Academy of Sciences. Reproduced with permission from ref. 69. Copyright 2019, Biochemistry.

efficient size for drug delivery and enhanced cellular uptake into the three types of cells: human embryonic kidney (HEK 293T) cells, human cervix carcinoma (HeLa) cells, and human breast cancer (MDA-MB-231) cells.[34] The latter with improved cellular uptake is critical for increasing drug delivery inside the target diseased cells.

Beyond these *in vitro* studies,[34,36] an *in vivo* experiment of using PX nanostructures have been demonstrated for potential anticancer immunotherapeutic recently.[72] Polyinosinic–polycytidylic acid (PolyIC-H) is a previously established potent anticancer immune adjuvant and a synthetic analog of double-stranded RNA, which is known to activate one of Toll-like receptors (TLR) such as TLR3. Through the activation of the TLR3, PolyIC-H can help to promote immune response inhibiting the growth of cancer cells. Although it is a potent anticancer immune adjuvant, it also comes with unfavorable systemic toxicity from enhanced type-I interferon release. In 2020, PX-based single-stranded RNA origami nanostructure were employed and investigated to reveal their potent anticancer immune stimulating activity using mice with peritoneally metastasized colorectal cancer as well as reduction in systemic toxicity due to type-I interferon production.[72] Unlike previously tested RNA nanostructures-based immune stimulators, this type of single-stranded RNA PX-based origami nanostructure did not require conjugation with lipids or other pattern-recognition receptors (PRR) moieties to activate immune response through Toll-like receptors pathways. For the *in vivo* experiment, three groups of the mice models received twice-a-week administration of a physiological buffer (phosphate-buffered saline, PBS) as a control group, PolyIC-H, and the RNA PX-based ssOrigami (RNA OG), respectively. Over the three weeks treatment, the tumor growth was imaged with florescence labeling of tumor cells (Fig. 8). The control group without containing any immune adjuvants, the tumor kept growing until the end point or the death of mice at day 16. In the other two test groups with RNA OG and PolyIC-H, the mice did not show any observable tumor growth, indicating that the two immune adjuvants effectively inhibited the growth of tumor. As for the mechanism of action by RNA OG, the study showed that RNA OG helps to reduce the activity of immune suppressing cells called myeloid-derived suppressor cells (MDSCs), which contains a high level of TGFβ, an immune inhibiting factor. On the contrary, RNA OG promotes the activity of *anti*-cancer immune response by T cells, NK cells, and dendritic cells

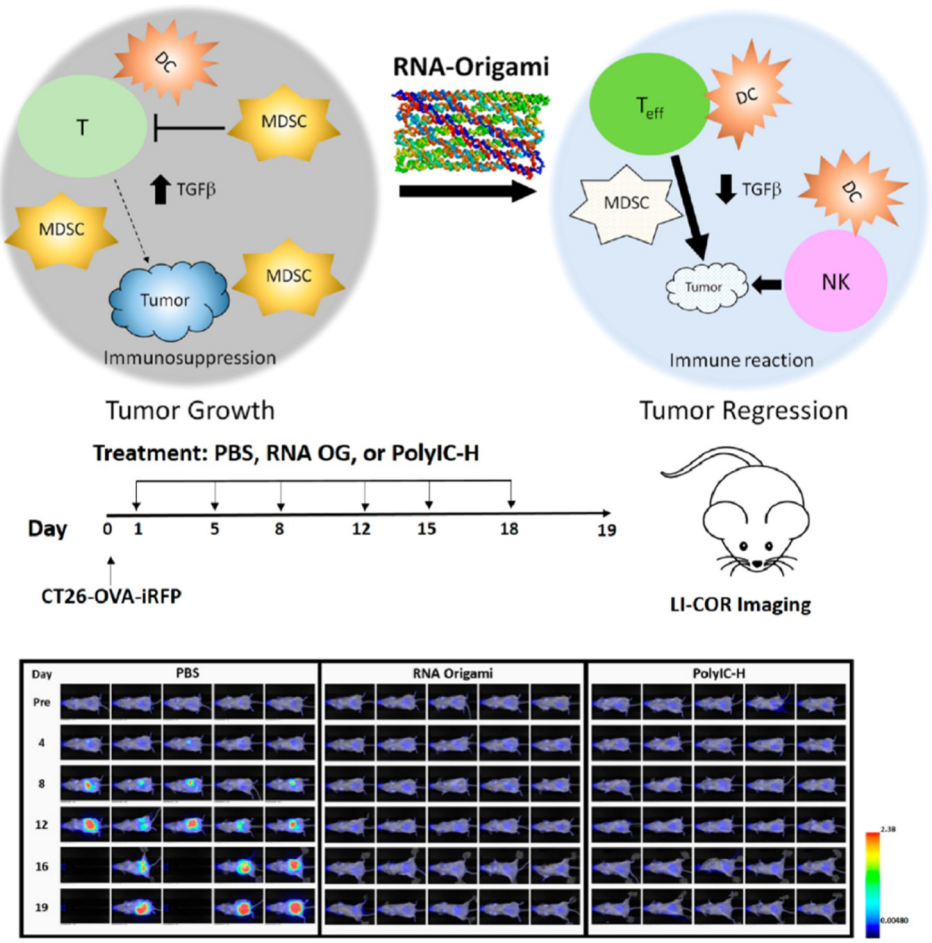

Fig. 8 The schematic of RNA-OG stimulates a potent innate response through a TLR3 pathway, and the comparison of antitumor adjuvant activity between RNA-OG and PolyIC *in vivo*. Reproduced with permission from ref. 72. Copyright 2020, ACS Nano.

(DC). This study provided an excellent *in vivo* biomedical application example, highlighting that PX motifs can be used to develop a potent anticancer immune adjuvant that is safe, potent, scalable, and cost-effective.

Discussion and outlook

In summary, this review paper discussed the general usage of PX motifs for nanoconstruction and bio-nanotechnological applications. For the nanoconstruction, comparing with AX-based multistranded nanostructures, the single-routed PX motifs does not require hundreds of staple strands leading to cost-reduction in synthesis of nanostructures and increase in the yield/reproducibility of well-formed target structures with high purity (not having excess multiple strands in the background). The single-routed PX motifs has enabled the construction of large, complex single-stranded nanostructures that are either highly knotted or unknotted. The 1D arrays with PX cohesive junctions were also shown to exhibit complex knotting features that strengthen chemical and nuclease resistance as well as addressability by arranging gold-nanoparticles on their surface. More importantly, the amplification of single strand routed PX motifs has several affordable and scalable methods including RCA, cellular amplification using phages, and SELEX with PCR. In addition, increasing the number of PX crossovers in a PX motif has improved the nuclease resistance, thus the biostability of the motif in the biological fluids. Next, the bio-nanotechnological applications of PX motifs have been discussed, including dynamic nanodevices enabled by adopting the two-state **PX-JX$_2$** rotary device, potentials for homology recognition, and biomedical applications *in vitro* and *in vivo*. The unique single-routing topology feature of PX motifs has allowed the creation of SELEX bivalent aptamer targeting thrombin as a potential anticoagulant and RCA-amplified PX-based single-stranded DNA nanostructures (ssDNs) in liposome sorting and enhancement of cellular uptake. Besides, the single-stranded RNA OG exhibited high biostability and reproducibility for anticancer immune stimulating activities *in vivo*.

Although we have introduced many exciting achievements of PX motifs, the challenges associated to PX motifs assembly still need more exploration. For example, Seeman and Fu's first introduced DAs generally has higher assembly yields than DPs,[20] suggesting that the optimization of designing and annealing rules for DPs assembly is necessary. Along the way, scientists found that providing a guided folding pathway to the PX motifs is critical in successful assembly. For instance, in 2008, Sherman's group tried to solve the low assembly yield problem of DPs by creating an optimized folding pathway.[29] They provided two case scenarios of inefficient folding pathways, strand end-pinning and junction-biased multimerization, based on the assignment of different hybridization sequence lengths between crossovers, leading to the low yield of DPs. In the strand end-pinning model, a DP motif was locked at the ends using long hybridization sequences, blocking one of the strands to weave through another to make crossovers. In junction-biased multimerization, the outer edges were instead all assigned with short hybridization sequences, leading to flexible crossovers and thus preferring to form multimers. Based on the two case scenarios, a clean assembly model was created with an optimized folding pathway, which successfully formed large 2D arrays. From this result, we can see that the folding pathway is a critical factor for the PX motifs assembly. However, this work only presents an example, further studies investigating new guided folding pathways through adjusting various parameters such as domain length, sequence design such as GC content, a nick position, and functionalized oligonucleotides would be highly desirable for general designing and annealing rules establishment to guarantee the formation yield of PX-based system.

One interesting study of PX folding pathways with functionalized oligonucleotides would be the incorporation of azobenzene-modified nucleic acids. For their excellent reversibility, photostability, and biofriendly feature (*e.g.* no waste generation), azobenzene-modified oligonucleotides have been useful in the development of dynamic, photoresponsive DNA nanomaterials.[73] Upon light radiation, azobenzene-modified oligonucleotide undergoes structural changes from *trans* state (a duplex form) to *cis* state (a dissociated single, stranded form) or *vice versa*. By introducing such dynamic, photoresponsive ability through azobenzene modification of nucleic acids, folding pathways of PX motifs can be guided and explored using light irradiation on the functionalized oligonucleotides.

Besides the double-crossover PX motifs, the folding mechanism of multi-PX crossover motifs can also be investigated. In fact, there are a limited number of studies testing parameters such as the number of crossovers[23] as well as the distance between them.[74] These studies used majorly gel and computer simulation to support their ideas. With more advanced tools such as high-resolution AFM imaging, Cryo-EM, and X-ray crystallography, more accurate details of the overall shape of PX motifs and even the individual bases of PX motifs with their relative orientations and locations to each other (using crystallography) can be revealed and utilized to promote the positive feedback loop between computer simulation and actual dataset. Such computer simulation tool incorporating a large library of actual PX motifs dataset would be highly promising in terms of time and cost savings related to the design/synthesis of PX motifs. All these efforts to understand the mechanism of PX motif formation will help to build a standardized set of rules for creating PX motifs with higher yields, allowing the use of PX motifs in practical applications to be explored further.

PX-based DNA nanostructures, with enhanced nuclease resistance, biostability, and prolonged drug circulation time in body, can function as novel drug-delivery system. As demonstrated in Chandrasekaran *et al.*'s study, adding PX crossovers to DNA nanostructures has great potential to significantly improve the biostability of nanostructures.[40] Further investigation of the biostability of PX motif will be highly useful to provide guidelines in the designing and optimization of PX structures suitable for biomedical applications. The impact of adding PX motifs on nuclease resistance of different systems,

such as tile-based arrays and origami structures, should be tested in comparison with similar AX systems systematically. By doing so, the advantages and disadvantages of using PX *versus* AX in different DNA nanostructures can be summarized and thus assist in the process of choosing which design strategy to be adopted in the construction of target nanostructures. Additionally, after characterizing the nuclease resistance of PX and AX systems, the two types of motifs can undergo ratio optimization to obtain the ideal level of nuclease resistance that is required for the programmed release (slow or fast) of drug molecules to target cells. Similar nuclease resistance comparison studies of introducing PX crossovers with other, previously established nuclease protection methods, such as chemical modifications,[75–78] protective coatings,[79–82] and solution treatments by the addition of nuclease inhibitors and temperature,[83] are required for better method determination in different applications including biosensing, bioimaging, and drug delivery.

In addition, a standardized, consistent criteria for biomedical applications to assess the nuclease resistance and biostability of various protection methods, including PX crossovers, are crucial.[84] The criteria should be comprehensive, to cover variables other than the protection methods themselves, such as type and concentration of a nuclease in the target biofluid, selection/preparation of biofluids, immune response, and *in vivo vs. in vitro* biostability, all of which are related to both nuclease resistance and biostability. The nuclease degradation mechanism is not completely understood, but studies have shown that many variables in the design of DNA nanostructures, such as DNA sequence,[85] groove features,[85] geometry,[86] backbone,[87] packing of helices,[88,89] number of nicks,[86] and PX crossovers[40] contribute to the degree of nuclease resistance. All the comparison studies suggested above for criteria standardization should contribute to understanding the variables associated with nuclease degradation mechanisms, thus clarifying previously unknown aspects of the nuclease mechanism.

With respect to biomedical and bionanotechnological applications, the use of PX motifs will be largely beneficial in many aspects. First, the RCA-amplified PX-based ssDNs can potentially be used to enhance the intracellular delivery of drug molecules targeting a variety of cancer cells after optimizing the size of liposomes through efficient liposome sorting. Investigation of pathways and final destinations after the intracellular uptake of the ssDN-coated liposomes, the optimal amount of ssDNs modified on liposomes, and selectivity towards cancer cells *versus* normal cells will be desirable to further reveal their potentials for effective anticancer activities. Second, specific PX-based bivalent aptamers with strong affinity to various disease-related proteins can be enriched and amplified *via* SELEX/PCR techniques. These aptamers not only can be used to modulate the activities of such proteins but also to detect the presence of such proteins as biosensors through labeling the aptamers with signaling molecules such as fluorescent probes.[90] Such enhanced binding of aptamers towards target molecules through multivalency with PX motifs should be explored more to improve sensitivity/selectivity in a variety of aptamer-based biosensing applications such as the detection of environmental toxins and disease biomarkers as well as food/drug quality control. Besides the applications with RCA and SELEX, use of PX motifs can introduce the benefits with cost-efficient scalability, dynamic features, and nuclease resistance/biostability to the other applications such as the development of: (1) Flexible and biostable nucleic acids-based molecular beacons[91] (*e.g.* imaging agents of small molecules such as RNA oligonucleotides *in vivo*). (2) Nuclease-resistant RNA-based therapeutics[92,93] involving messenger RNA (mRNA, *e.g.* COVID vaccines), short or small interfering RNA involved in RNA interference, RNAi, (siRNA, *e.g.* pathogen infection treatment and diseased protein expression control), antisense RNA oligonucleotides (ASOs, *e.g.* regulation of protein expression for disease treatment), and guide RNAs (gRNAs, *e.g.* Clustered Regularly Interspersed Short Palindromic Repeats (CRISPR) gene therapy and RNA editing technology[94]). Being biocompatible, biostable, and nuclease-resistant, PX motifs employed in small DNA/RNA molecules from molecular beacons and RNA therapeutics can protect the small molecules from nuclease degradation and also eliminate the need for the incorporation of nuclease-resistant, chemically modified nucleotides (*e.g.* 2′-*O*-methyl modifications), which may produce toxicity and change the effectiveness of the molecules when used in large amounts.[93,95]

Overall, PX motifs are intrinsic stable motifs as shown in the creation of large-sized complex single-stranded nanostructures, and they are less studied in comparison to AX motifs allowing more design and research space. Considering all the benefits, PX motifs will be highly useful molecular building blocks in a variety of applications. Future studies highlighted in this section hold a great promise for building generalized rules to create stable PX-based nanostructures, assessing/optimizing PX-based nuclease resistance, and introducing the advantages of using PX motifs into actual examples of bionanotechnological and biomedical applications.

Conflicts of interest

There are no conflicts to declare.

Acknowledgements

This work is supported by a US National Science Foundation (NSF) Faculty Early Career Development Award (DMR-2046835), an NSF grant (CCF-2007821), a Busch Biomedical Grant, and a faculty Startup Fund from Rutgers University.

References

1 W. Liu, X. Wang, T. Wang, R. Sha and N. C. Seeman, *Nano Lett.*, 2008, **8**, 317–322.
2 Y. P. Ohayon, R. Sha, O. Flint, W. Liu, B. Chakraborty, H. K. K. Subramanian, J. Zheng, A. R. Chandrasekaran,

H. O. Abdallah, X. Wang, X. Zhang and N. C. Seeman, *ACS Nano*, 2015, **9**, 10304–10312.
3 E. Winfree, F. Liu, L. A. Wenzler and N. C. Seeman, *Nature*, 1998, **394**, 539–544.
4 H. Yan, S. H. Park, G. Finkelstein, J. H. Reif and T. H. LaBean, *Science*, 2003, **301**, 1882–1884.
5 W. Shen, Q. Liu, B. Ding, Z. Shen, C. Zhu and C. Mao, *Org. Biomol. Chem.*, 2016, **14**, 7187–7190.
6 P. W. K. Rothemund, *Nature*, 2006, **440**, 297–302.
7 S. M. Douglas, H. Dietz, T. Liedl, B. Högberg, F. Graf and W. M. Shih, *Nature*, 2009, **459**, 414–418.
8 W. M. Shih, J. D. Quispe and G. F. Joyce, *Nature*, 2004, **427**, 618–621.
9 M. Chang, C.-S. Yang and D.-M. Huang, *ACS Nano*, 2011, **5**, 6156–6163.
10 S. Li, Q. Jiang, S. Liu, Y. Zhang, Y. Tian, C. Song, J. Wang, Y. Zou, G. J. Anderson, J.-Y. Han, Y. Chang, Y. Liu, C. Zhang, L. Chen, G. Zhou, G. Nie, H. Yan, B. Ding and Y. Zhao, *Nat. Biotechnol.*, 2018, **36**, 258–264.
11 R. Hu, X. Zhang, Z. Zhao, G. Zhu, T. Chen, T. Fu and W. Tan, *Angew. Chem., Int. Ed.*, 2014, **53**, 5821–5826.
12 X. Liu, Y. Xu, T. Yu, C. Clifford, Y. Liu, H. Yan and Y. Chang, *Nano Lett.*, 2012, **12**, 4254–4259.
13 D. Jiang, Y. Sun, J. Li, Q. Li, M. Lv, B. Zhu, T. Tian, D. Cheng, J. Xia, L. Zhang, L. Wang, Q. Huang, J. Shi and C. Fan, *ACS Appl. Mater. Interfaces*, 2016, **8**, 4378–4384.
14 H.-M. Meng, X. Zhang, Y. Lv, Z. Zhao, N.-N. Wang, T. Fu, H. Fan, H. Liang, L. Qiu, G. Zhu and W. Tan, *ACS Nano*, 2014, **8**, 6171–6181.
15 A. Prokup, J. Hemphill and A. Deiters, *J. Am. Chem. Soc.*, 2012, **134**, 3810–3815.
16 R. Freeman, T. Finder and I. Willner, *Angew. Chem., Int. Ed.*, 2009, **48**, 7818–7821.
17 M. R. Jones, N. C. Seeman and C. A. Mirkin, *Science*, 2015, **347**, 1260901.
18 D. Wang, J. Cui, M. Gan, Z. Xue, J. Wang, P. Liu, Y. Hu, Y. Pardo, S. Hamada, D. Yang and D. Luo, *J. Am. Chem. Soc.*, 2020, **142**, 10114–10124.
19 K. E. Bujold, A. Lacroix and H. F. Sleiman, *Chem*, 2018, **4**, 495–521.
20 T. J. Fu and N. C. Seeman, *Biochemistry*, 1993, **32**, 3211–3220.
21 X. Li, X. Yang, J. Qi and N. C. Seeman, *J. Am. Chem. Soc.*, 1996, **118**, 6131–6140.
22 D. Han, S. Pal, J. Nangreave, Z. Deng, Y. Liu and H. Yan, *Science*, 2011, **332**, 342–346.
23 Z. Shen, H. Yan, T. Wang and N. C. Seeman, *J. Am. Chem. Soc.*, 2004, **126**, 1666–1674.
24 D. Han, X. Qi, C. Myhrvold, B. Wang, M. Dai, S. Jiang, M. Bates, Y. Liu, B. An, F. Zhang, H. Yan and P. Yin, *Science*, 2017, 358.
25 X. Qi, F. Zhang, Z. Su, S. Jiang, D. Han, B. Ding, Y. Liu, W. Chiu, P. Yin and H. Yan, *Nat. Commun.*, 2018, **9**, 4579.
26 X. Zhang, H. Yan, Z. Shen and N. C. Seeman, *J. Am. Chem. Soc.*, 2002, **124**, 12940–12941.
27 D. Ackermann, S. S. Jester and M. Famulok, *Angew. Chem., Int. Ed.*, 2012, **51**, 6771–6775.
28 Y. P. Ohayon, R. Sha, O. Flint, A. R. Chandrasekaran, H. O. Abdallah, T. Wang, X. Wang, X. Zhang and N. C. Seeman, *ACS Nano*, 2015, **9**, 10296–10303.
29 M. T. Kumara, D. Nykypanchuk and W. B. Sherman, *Nano Lett.*, 2008, **8**, 1971–1977.
30 W. Shen, Q. Liu, B. Ding, C. Zhu, Z. Shen and N. C. Seeman, *Org. Biomol. Chem.*, 2017, **15**, 465–469.
31 X. Wang, A. R. Chandrasekaran, Z. Shen, Y. P. Ohayon, T. Wang, M. E. Kizer, R. Sha, C. Mao, H. Yan, X. Zhang, S. Liao, B. Ding, B. Chakraborty, N. Jonoska, D. Niu, H. Gu, J. Chao, X. Gao, Y. Li, T. Ciengshin and N. C. Seeman, *Chem. Rev.*, 2019, **119**, 6273–6289.
32 S. Kosuri and G. M. Church, *Nat. Methods*, 2014, **11**, 499–507.
33 C. Lin, X. Wang, Y. Liu, N. C. Seeman and H. Yan, *J. Am. Chem. Soc.*, 2007, **129**, 14475–14481.
34 Y. Jia, L. Chen, J. Liu, W. Li and H. Gu, *Chem*, 2021, **7**, 959–981.
35 C. Lin, S. Rinker, X. Wang, Y. Liu, N. C. Seeman and H. Yan, *Proc. Natl. Acad. Sci. U. S. A.*, 2008, **105**, 17626–17631.
36 Y. Zhou, X. Qi, Y. Liu, F. Zhang and H. Yan, *ChemBioChem*, 2019, **20**, 2494–2503.
37 A. R. Chandrasekaran, M. Macisaac, P. Dey, O. Levchenko, L. Zhou, M. Andres, B. K. Dey and K. Halvorsen, *Sci. Adv.*, 2019, **5**, e72.
38 D. Bhatia, S. Surana, S. Chakraborty, S. P. Koushika and Y. Krishnan, *Nat. Commun.*, 2011, **2**, 339.
39 W. Yang, *Q. Rev. Biophys.*, 2011, **44**, 1–93.
40 A. R. Chandrasekaran, J. Vilcapoma, P. Dey, S. W. Wong-Deyrup, B. K. Dey and K. Halvorsen, *J. Am. Chem. Soc.*, 2020, **142**, 6814–6821.
41 A. Idili, A. Vallee-Belisle and F. Ricci, *J. Am. Chem. Soc.*, 2014, **136**, 5836–5839.
42 C. Mao, W. Sun, Z. Shen and N. C. Seeman, *Nature*, 1999, **397**, 144–146.
43 V. Viasnoff, A. Meller and H. Isambert, *Nano Lett.*, 2006, **6**, 101–104.
44 X. Liang, H. Nishioka, N. Takenaka and H. Asanuma, *ChemBioChem*, 2008, **9**, 702–705.
45 W. Shen, M. F. Bruist, S. D. Goodman and N. C. Seeman, *Angew. Chem., Int. Ed.*, 2004, **43**, 4750–4752.
46 B. Yurke, A. J. Turberfield, A. P. Mills, F. C. Simmel and J. L. Neumann, *Nature*, 2000, **406**, 605–608.
47 F. C. Simmel and B. Yurke, *Phys. Rev. E: Stat., Nonlinear, Soft Matter Phys.*, 2001, **63**, 041913.
48 F. C. Simmel and B. Yurke, *Appl. Phys. Lett.*, 2002, **80**, 883–885.
49 W. B. Sherman and N. C. Seeman, *Nano Lett.*, 2004, **4**, 1203–1207.
50 H. Yan, X. Zhang, Z. Shen and N. C. Seeman, *Nature*, 2002, **415**, 62–65.
51 B. Chakraborty, R. Sha and N. C. Seeman, *Proc. Natl. Acad. Sci. U. S. A.*, 2008, **105**, 17245–17249.
52 S. Liao, *Science*, 2004, **306**, 2072–2074.
53 B. Chakraborty, N. Jonoska and N. C. Seeman, *Chem. Sci.*, 2012, **3**, 168–176.

54 B. Ding and N. C. Seeman, *Science*, 2006, **314**, 1583–1585.
55 H. Gu, J. Chao, S. J. Xiao and N. C. Seeman, *Nature*, 2010, **465**, 202–205.
56 X. Wang, X. Zhang, C. Mao and N. C. Seeman, *Proc. Natl. Acad. Sci. U. S. A.*, 2010, **107**, 12547–12552.
57 E. U. Selker, *Annu. Rev. Genet.*, 1990, **24**, 579–613.
58 M. S. Apte and V. H. Meller, *Genet. Res. Int.*, 2012, **2012**, 430587.
59 E. F. Joyce, N. Apostolopoulos, B. J. Beliveau and C. T. Wu, *PLoS Genet.*, 2013, **9**, e1004013.
60 L. Mlynarova, R. C. Jansen, A. J. Conner, W. J. Stiekema and J. P. Nap, *Plant Cell*, 1995, **7**, 599–609.
61 T. Hassold and P. Hunt, *Nat. Rev. Genet.*, 2001, **2**, 280–291.
62 T. R. Strick, V. Croquette and D. Bensimon, *Proc. Natl. Acad. Sci. U. S. A.*, 1998, **95**, 10579–10583.
63 J. Nishikawa and T. Ohyama, *Nucleic Acids Res.*, 2013, **41**, 1544–1554.
64 C. Danilowicz, C. H. Lee, K. Kim, K. Hatch, V. W. Coljee, N. Kleckner and M. Prentiss, *Proc. Natl. Acad. Sci. U. S. A.*, 2009, **106**, 19824–19829.
65 S. Inoue, S. Sugiyama, A. A. Travers and T. Ohyama, *Biochemistry*, 2007, **46**, 164–171.
66 G. S. Baldwin, N. J. Brooks, R. E. Robson, A. Wynveen, A. Goldar, S. Leikin, J. M. Seddon and A. A. Kornyshev, *J. Phys. Chem. B*, 2008, **112**, 1060–1064.
67 S. McGavin, *J. Mol. Biol.*, 1971, **55**, 293–298.
68 J. H. Wilson, *Proc. Natl. Acad. Sci. U. S. A.*, 1979, **76**, 3641–3645.
69 M. Kizer, I. D. Huntress, B. D. Walcott, K. Fraser, C. Bystroff and X. Wang, *Biochemistry*, 2019, **58**, 1332–1342.
70 P. Liu, G. Chen and J. Zhang, *Molecules*, 2022, **27**, 1372–1394, DOI: **10.3390/molecules27041372**.
71 R. J. Banga, N. Chernyak, S. P. Narayan, S. T. Nguyen and C. A. Mirkin, *J. Am. Chem. Soc.*, 2014, **136**, 9866–9869.
72 X. Qi, X. Liu, L. Matiski, R. Rodriguez Del Villar, T. Yip, F. Zhang, S. Sokalingam, S. Jiang, L. Liu, H. Yan and Y. Chang, *ACS Nano*, 2020, **14**, 4727–4740.
73 C. Wang, M. P. O'Hagan, Z. Li, J. Zhang, X. Ma, H. Tian and I. Willner, *Chem. Soc. Rev.*, 2022, **51**, 720–760.
74 E. Poppleton, J. Bohlin, M. Matthies, S. Sharma, F. Zhang and P. Šulc, *Nucleic Acids Res.*, 2020, **48**, e72–e72.
75 J. W. Conway, C. K. McLaughlin, K. J. Castor and H. Sleiman, *Chem. Commun.*, 2013, **49**, 1172–1174.
76 V. Cassinelli, B. Oberleitner, J. Sobotta, P. Nickels, G. Grossi, S. Kempter, T. Frischmuth, T. Liedl and A. Manetto, *Angew. Chem., Int. Ed.*, 2015, **54**, 7795–7798.
77 C. Lin, Y. Ke, Z. Li, J. H. Wang, Y. Liu and H. Yan, *Nano Lett.*, 2009, **9**, 433–436.
78 Q. Liu, G. Liu, T. Wang, J. Fu, R. Li, L. Song, Z. G. Wang, B. Ding and F. Chen, *ChemPhysChem*, 2017, **18**, 2977–2980.
79 A. Lacroix, T. G. W. Edwardson, M. A. Hancock, M. D. Dore and H. F. Sleiman, *J. Am. Chem. Soc.*, 2017, **139**, 7355–7362.
80 S. D. Perrault and W. M. Shih, *ACS Nano*, 2014, **8**, 5132–5140.
81 S. T. Wang, M. A. Gray, S. Xuan, Y. Lin, J. Byrnes, A. I. Nguyen, N. Todorova, M. M. Stevens, C. R. Bertozzi, R. N. Zuckermann and O. Gang, *Proc. Natl. Acad. Sci. U. S. A.*, 2020, **117**, 6339–6348.
82 M.-K. Nguyen, V. H. Nguyen, A. K. Natarajan, Y. Huang, J. Ryssy, B. Shen and A. Kuzyk, *Chem. Mater.*, 2020, **32**, 6657–6665.
83 J. Hahn, S. F. J. Wickham, W. M. Shih and S. D. Perrault, *ACS Nano*, 2014, **8**, 8765–8775.
84 A. R. Chandrasekaran, *Nat. Rev. Chem.*, 2021, **5**, 225–239.
85 D. Suck, *Biopolymers*, 1997, **44**, 405–421.
86 J. W. Keum and H. Bermudez, *Chem. Commun.*, 2009, 7036–7038, DOI: **10.1039/b917661f**.
87 A. Lacroix, E. Vengut-Climent, D. de Rochambeau and H. F. Sleiman, *ACS Cent. Sci.*, 2019, **5**, 882–891.
88 S. Goltry, N. Hallstrom, T. Clark, W. Kuang, J. Lee, C. Jorcyk, W. B. Knowlton, B. Yurke, W. L. Hughes and E. Graugnard, *Nanoscale*, 2015, **7**, 10382–10390.
89 C. E. Castro, F. Kilchherr, D. N. Kim, E. L. Shiao, T. Wauer, P. Wortmann, M. Bathe and H. Dietz, *Nat. Methods*, 2011, **8**, 221–229.
90 A. Hanif, R. Farooq, M. U. Rehman, R. Khan, S. Majid and M. A. Ganaie, *Saudi Pharm. J.*, 2019, **27**, 312–319.
91 K. Wang, Z. Tang, C. J. Yang, Y. Kim, X. Fang, W. Li, Y. Wu, C. D. Medley, Z. Cao, J. Li, P. Colon, H. Lin and W. Tan, *Angew. Chem., Int. Ed.*, 2009, **48**, 856–870.
92 D. Kim and J. Rossi, *Biotechniques*, 2008, **44**, 613–616.
93 S. Bajan and G. Hutvagner, *Cells*, 2020, **9**, 137–163, DOI: **10.3390/cells9010137**.
94 S. Reardon, *Nature*, 2020, **578**, 24–27.
95 S. M. Davis, J. Sousa, L. Vangjeli, M. R. Hassler, D. Echeverria, E. Knox, A. A. Turanov, J. F. Alterman and A. Khvorova, *Mol. Ther.–Nucleic Acids*, 2020, **21**, 266–277.

